Potential Complementary Value of Noncontrast and Contrast Enhanced CT Radiomics in Colorectal Cancers

Bogdan Badic, Marie Charlotte Desseroit, Mathieu Hatt, Dimitris Visvikis

Potential complementary value of non contrast and contrast enhanced CT radiomics in colorectal cancers

Bogdan Badic[1]*, Marie Charlotte Desseroit[1], Mathieu Hatt[1¶], Dimitris Visvikis[1¶]

[¶] These authors contributed equally to this work.

INSERM, UMR 1101, LaTIM, CHRU Morvan, 2 Avenue Foch, 29200 Brest, France

*** Corresponding author**

Bogdan Badic

E-mail: bogdan.badic@chu-brest.fr

[1]INSERM, UMR 1101, LaTIM, CHRU Morvan, 2 Avenue Foch, 29200 Brest, France

Abstract

Rationale and Objectives: The aim of our study was to assess the relationships between textural features extracted from contrast enhanced (CE) and non-contrast enhanced (NCE) computed tomography (CT) images of primary colorectal cancer (CRC), in order to identify radiomics features more likely to provide potential complementary information regarding outcome.

Materials and methods: Sixty-one patients with primary CRC underwent both CE-CT and NCE-CT scans within the same acquisition. First-order and textural features (with three different methods for grey-level discretization) were extracted from the tumor volume in both modalities and their correlation was assessed with Spearman's rank correlation (rs). Significance was assessed at $P<0.05$ with correction for multiple comparisons**.** Kaplan-Meier estimation and log-rank tests were used to identify features associated with long term patient survival.

Results: moderate positive correlations were observed between CE-CT and NCE-CT histogram-derived entropy ($Entropy_{Hist}$) and area under the curve (CH_{AUC}) (rs=0.49, P<0.001 and rs= 0.45, P<0.001, respectively). Some 2^{nd} and 3^{rd} order textural features were found highly correlated between CE-CT and NCE-CT, such as small zone-size emphasis (SZSE) (rs=0.729, P<0.001) and zone-size percentage (SZP) (rs=0.770, P<0.001). Grey-levels discretization methods influenced these correlations. A few of the third order NCE-CT and CE-CT features were significantly associated with survival.

Conclusion: Some radiomics features with moderate correlations between non enhanced and enhanced CT images were found to be associated with survival, thus

suggesting that complementary prognostic value may be extracted from both modalities when available.

Keywords: colorectal cancer; computed tomography; radiomics; tumor heterogeneity;

Introduction

Colorectal cancer (CRC) is a major public health issue, being the third most commonly diagnosed cancer and the fourth cause of death by cancer worldwide ([1]). Although the diagnosis of CRC is always based on visually guided flexible colonoscopy, which is the only technique that provides a histopathological diagnosis, the pretreatment assessment of the disease also involves visual analysis of computed tomography (CT) images.

Colorectal carcinoma, the most common cancer of the gastrointestinal tract, is characterized by marked intra-tumor genetic heterogeneity ([2]). Tumor heterogeneity may be (at least partly) quantitatively assessed on routinely acquired CT scans using radiomics. Radiomics consists in describing a segmented tumor region using a number of quantitative features derived from image data ([3,4,5]). Texture analysis performed on CT images quantifies the spatial and intensity relationships between the grey levels of voxels. A number of textural features (TFs) can be calculated that could provide a measure of tumor heterogeneity at the imaging macroscopic scale ([6]). For most of the TFs usually extracted in the radiomics workflow, there are no clear correlations with underlying intra-tumor genetic or histopathology modifications yet. However, it has been suggested that radiomics features extracted from unenhanced CT (NCE-CT) may refer to the variability in tissue densities that could

result from spatially varying fibrosis, cell density and/or necrosis ([5,7]). Similarly, in contrast-enhanced CT (CE-CT) images, radiomics features may be associated more specifically with the spatial variability in microvessels density ([8]).

Several studies have investigated the potential clinical value of CT radiomics features in CRC. Higher (respectively lower) values of entropy (respectively uniformity) derived from intensity histogram calculated in various sub-volumes obtained by filtering hepatic perfusion CT images may predict poorer survival for CRC patients ([9,10]). Other radiomics features, including entropy, standard deviation and skewness derived from intensity histograms were found to be significantly associated with tumor grade and KRAS mutation in untreated CRC liver metastases ([11]). CT images analysis through fractal dimension was found to provide metrics differentiating benign from malignant metastatic lymph nodes in CRC ([12]). A radiomics signature containing 16 features derived from CT images was also found to be correlated with the preoperative staging of CRC ([13]).

The majority of CRC studies used the portal phase of CT imaging for radiomics features analysis. In order to identify which radiomics features are likely to potentially provide complementary information for the characterization of CRC tumors from CE-CT compared to NCE-CT, the first step is to investigate the changes induced by contrast administration. This can be performed by determining the levels of correlation between features extracted from the two images. When both modalities are available, features with low levels of correlation could be considered as potentially complementary to quantify different patterns thus providing different information. The second step is to investigate the usefulness of features for predicting the outcome of patients.

The aim of our study was thus to assess the correlation relationships between features extracted from CE-CT and NCE-CT images and their potential complementary prognostic value. Given the relatively small cohort available, our primary objective was to investigate the correlation between features extracted from CE-CT and NCE-CT images and survival, not to train and validate a full multivariate prognostic model, which will be the focus of future investigations in a larger prospective cohort currently being recruited.

Materials and Methods

Patients cohort

This retrospective study was approved by our institutional review board and the informed consent requirement was waived. We retrospectively collected the clinical, histopathological and imaging data from 61 patients who were pathologically diagnosed with colorectal cancer at our institution between January 2010 and December 2016. There were 17 rectal and 44 colon adenocarcinoma. For all patients localization of the tumor had been performed during colonoscopy and the tumor was visible on the CT images. The extent (size) of the tumor (T), regional lymph node involvement (N) and the presence or absence of distant metastases (M) was assessed by postsurgical histopathology results and the UICC TNM classification of colorectal tumors was used for staging ([14]). The survival time in months, from the time of surgery to death or last visit, was available for all patients.

CT imaging

As part of the routine imaging protocol at our institution, patients underwent both CE and NCE abdominal CT acquisitions carried out before surgery or previous systemic treatment (radiotherapy/chemotherapy). The portal venous phase and NCE CT images were exploited for the present analysis. Both CE-CT and NCE-CT were acquired covering the same axial extent, during the same acquisition session and in the same scanner for each patient, using the same reconstruction settings (slice thickness and matrix size), reducing any potential misregistration issue between the two datasets. Scans were performed on a Siemens Definition AS64 (Siemens medical, Erlangen, Germany). Standard acquisition settings were: tube voltage 120 kVp, automatic tube current–exposure time product, 0.5 s rotation time, 1.25 mm slice thickness, matrix size 512×512 pixels and inspiratory breath hold. Intravenous contrast (Xenetix 350; Guebert, Roissy, France) was administered at a 3 mL/sec injection rate with a pump injector (Medrad Stellant ; Bayer, NY). A typical set of CE-CT and NCE-CT scans for one patient is shown in Fig.1.

Fig 1. (a-c) NCE-CT and (b-d) CE-CT images of a patient with colonic adenocarcinoma

Radiomics analysis

Only primary tumors previously identified were analyzed. The previously validated approach exploiting the 3D Slicer™ software ([15]) was used to semi-automatically delineate morphological tumor volumes in 3D on the portal phase CT images by an experienced specialist. Since the acquisition of both NCE and CE-CT

images was carried out during the same examination, no image registration was necessary, and it allowed to automatically report the segmentation performed by the expert on CE images on the associated NCE images within 3D slicer. This ensured avoiding differences between features occurring from different segmentations shape and volumes.

Radiomics features were extracted in 3D from the segmented volumes and implemented in-house following the most up-to-date definitions and guidelines from the Imaging Biomarkers Standardization Initiative (IBSI). Features values were validated against the digital phantom values provided in the IBSI harmonization study ([16]). The usual radiomics features were considered: first order statistics consist of measurements from the histogram of voxel intensity values contained within the volume of interest. As such, they do not take into account spatial relationships between voxels. Second order features are calculated from grey-level co-occurrence matrix (GLCM) which provides a representation of relationships between neighboring voxels, at a local scale of a given voxels and its direct neighbors. Third order features are more complex as they characterize relationships between voxels at a regional scale (i.e., groups of voxels of different sizes depending on the considered texture matrix) ([17]). They are calculated from the neighborhood grey-tone difference matrix (NGTDM), the grey-level run length matrix (GLRLM) and the grey-level size zone matrix (GLSZM). Mathematical definitions and equations for features assessed in our study can be found in the Appendix.

Shape descriptors were not included in the analysis because the segmentation of the tumor volumes was only performed once on the CE-CT and reported to the NCE-CT, thus volume and shape features are exactly the same in both images. No filter-based analysis (either textural features on wavelet decompositions ([5]) or

histogram-analysis in sub-volumes identified by log of Laplacian filters ([18])) was included to limit the number of considered features. The intensities in the native images were discretized before building second and third order textural matrices. It has been shown that this step can have a significant impact on the TFs values and distributions ([19]). We chose to include the two most often used techniques (i.e. into a fixed number of bins and into fixed bin width) for discretization, as well as histogram equalization that was actually suggested in the *princeps* paper by Haralick ([19]), for completeness. Three different sets of TFs (denoted from here onwards as L, E and R) were thus generated according to a discretization into a fixed number of bins (64) using either a uniform distribution (L) of the original Hounsfield units (HU) (equation 1 in the appendix) or a histogram equalization (E) (equation 2 in the appendix), as well as into a variable number of bins of fixed width (R), for instance 10 HU (equation 3 in the appendix) ([19]).

Statistical analysis

Statistical analyses were performed using IBM *SPSS* Statistics V 20.0.0 software (IBM Corp. Released 2011. IBM SPSS Statistics for Windows, Version 20.0. Armonk, NY: IBM Corp.). Correlations between features were quantified using Spearman's rank coefficient (rs). Correction for multiple testing with the Bonferroni method was applied and consequently a p-value<0.000641 (=0.05/78) was considered significant. The receiver operating characteristics (ROC) curves were generated and the optimal cutoff threshold values were determined according to Youden's index ([20]) (supplementary material 2.) Prognostic value of each feature for the survival was assessed using the Kaplan-Meier method and associated log-rank test, with cut-off thresholds previously determined .

Results

Patient characteristics

There were 61 patients (40 male, 21 female), mean age 70 years (range 25-93). According to UICC staging there were 5 stage I tumors, 3 stage II tumors, 36 stage III tumors and 17 stage IV tumors. Of these, 17 were in the rectum, 17 in the left colon, 3 in the transverse colon and 24 in the right colon.

Table 1. ROC analysis and Log-rank test p-values for clinical parameters

Fig.2 Kaplan Meyer survival curve with Log Rank for Stage

Correlation and survival analysis

Clinical parameters

All available clinical and pathological parameters (age, T and M stage, UICC stage, lymphovascular invasion) but N stage and histological grade, were found significantly associated with survival (p-value <0.001).

First-order metrics

Table 2. Spearman rank correlation between CE and NCE-CT first order features [after Bonferonni correction (*p-value* <0.000641 (=0.05/78)]

The features histogram-derived skeweness, maximum, entropy ($Entropy_{HIST}$) and area under the curve of the cumulative histogram (CH_{AUC}) showed moderate positive correlations between CE-CT and CT ($Entropy_{Hist}$ *rs*= 0.49, AUC *rs*= 0.41,

P<0.00006) (Fig 2). None of the first order features was significantly associated with survival.

Fig 3. $Entropy_{HIST}$ and CH_{AUC} distributions in NCE-CT and CE-CT

Second-order metrics

Table 3. Spearman rank correlation between CE and NCE-CT second order features [after Holm-Bonferonni correction (*p-value* <0.000641 (=0.05/78)]

Strong correlations were found for two second order metrics, namely Inverse difference (ID_R) (*rs*=0.72) and inverse difference moment (IDM_R) (*rs*= 0.74), both with P<0.00000001. For all other second-order features, only low to moderate levels of correlations (rs between 0.1 and 0.62) were observed.

It is important to emphasize on the impact of the discretization step for textural features (Fig 3). For example, Inverse difference (ID), sum of square variance (SOSV) and sum average (SAVE) exhibited much lower correlations between CE-CT and NCE-CT when calculated after fixed-width bins discretization (rs=0.21, 0.1 and 0.19) than after histogram equalization discretization (rs=0.72, 0.54 and 0.54). On the contrary, for $entropy_{GLCM}$, moderate correlations were observed whatever the discretization method: rs=0.42, *rs*=0.55 and *rs*=0.60 for L, E and R discretization respectively, P<0.00001.

Second order features were not significantly correlated with survival after Bonferroni correction, despite a trend for sum entropy ($SENT_L$), inverse difference moment ($IDM_{R)}$ and Inverse difference ($ID_{R)}$ extracted from NCE-CT.

Fig 4. IDM (inverse difference moment) and ID (inverse difference) distribution using different discretization approaches (L-linear, E-equalization and R-fixed-width bins)

Third-Order Metrics

Table 3. Spearman rank correlation between CE and NCE-CT third order features [after Holm-Bonferonni correction (*p-value* <0.000641 (=0.05/78)]

The features that exhibited the highest correlations between CE and NCE-CT were Small-zone-size emphasis ($SZSE_R$) (*rs*=0.729), Large-zone-size emphasis ($LZSE_R$) (*rs*=0.789), Zone-size percentage (ZSP_R) (*rs*=0.770), Zone-size nonuniformity ($ZSNU_{E,R}$) (*rs*=0.784; *rs*=0.709) and Gray-level nonuniformity (GLNU) (*rs*=0.789). The other 3rd order features exhibited low to moderate correlations (r between 0.15 and 0.65). Correlative relationships of the textural features Small-zone-size emphasis (SZSE) and Zone-size percentage (ZSP) according to the different discretizations schemes (L-linear, E-equalization, R-fixed-width bins) are illustrated in Fig.5.

Fig 5. Illustrations of correlative relationships of textural feature SZSE and ZSP on different quantization approaches (L-linear, E-equalization, R-fixed-width bins)

Amongst third order features, several NCE-CT features [(High-gray-level-zone emphasis ($HGLZE_E$), Small-zone/high-gray emphasis ($SZHGE_L$), Zone-size nonuniformity ($ZSNU_R$), Gray-level nonuniformity ($GLNU_{L,\ R}$)] and CE-CT features [(Small-zone /low-gray emphasis ($SZLGE_R$), Low-gray-level-zone emphasis ($LGLZE_L$), Low Gray-level Run Emphasis ($LGRE_L$)] were found to be significantly associated with survival after correction for multiple testing.

Kaplan-Meier survival analysis

No first or second order radiomics were found to show significantly different survival distributions. Some CE and NCE-CT third order features were correlated with survival (see below). Amongst those features associated with survival, two categories can be distinguished according to their level of correlation between NCE and CE-CT..

One CE-CT feature $SZLGE_R$ (*rs*=0.46, P<0.0001) and three NCE-CT features $ZSNU_R$ (*rs*=0.70, P<0.0001), $GLNU_L$ (*rs*=0.64, P<0.0001) and $GLNU_R$ (*rs*=0.65, P<0.0001) correlated on Spearman analysis were found also to be associated with survival (p<0.006). NCE-CT features $HGLZE_E$ (*rs*=0.14, P<0.253); $SZHGE_L$ (*rs*=0.33, P<0.009) and CE-CT features $LGLZE_L$ (*rs*=0.37, P<0.002); $LGRE_L$ (*rs*=0.31, P<0.01) were not correlated on Spearman analysis but were found to be prognostic of survival (p<0.006). Two moderately correlated texture features ($SZLGE_R$ and $ZSNU_R$) (*rs*=0.46, P<0.0001 and *rs*=0.70, P<0.0001, respectively) had significant association with survival after Bonferroni correction (p value<0.01) for both NCE and CE-CT (Fig.6).

Fig.6 Kaplan Meyer survival curves with Log Rank for CE and NCE-CT features $SZLGE_R$ and $ZSNU_R$

Some radiomics features identified as prognostic factors were however also correlated with clinical factors. T stage was correlated with NCE-CT feature $SZLGE_R$ (p<0.046), M stage with NCE-CT feature $SZLGE_R$ (p<0.009) and lymphovascular invasion was correlated with NCE-CT feature $HGLZE_E$ (P<0.023). Histological grade, N stage and UICC stage on the other hand were not found to be correlated to any of the radiomics features.

Discussion

Malignant tumors present spatial and temporal heterogeneity in their biological characteristics and behavior. Several studies have identified radiomics features as prognostic and predictive factors of disease and associated with treatment outcomes ([8,11,21]). This study evaluated the potential complementary value of radiomics features extracted from contrast enhanced and non-contrast enhanced CT images for predicting the survival outcome of patients with primary colorectal tumors.

Our analysis based on Spearman's rank correlation identified several histogram-derived features (skewness, maximum, entropy ($Entropy_{HIST}$), CH_{AUC}) to be moderately correlated between the two image modalities. Miles, *et al*. showed that $entropy_{hist}$ from CE-CT scans correlated with overall survival of colorectal liver metastases ([22]). Lubner, *et al*. performed also filter-based histogram analysis of colorectal hepatic metastatic lesions on pre-treatment CE-CT scans in 77 patients and identified $entropy_{hist}$ as a prognostic factor ([11]). Our study failed to identify correlations between the first order features and overall survival. This could potentially be explained by the fact that global features extracted from the intensity histogram characterize the distribution of the voxel intensities without taking into consideration spatial relationships between the voxels ([23]). This is similar to filter-based histogram analysis, except in the present case it is performed in the entire tumor-volume instead of various sub-volumes determined by filtering at various scales that may better highlight parts of the tumor with specific patterns ([18]).

Discretization is an important factor to consider for second- and third-order texture metrics. For instance, the repeatability of features is also affected by the discretization choices ([24,25]). In the present study, we showed the observed levels of correlation could depend on the chosen discretization method, as the correlation between CE and NCE-CT for several parameters (SZSE, LZSE, LGLZE, SZLGE, LZLGE, LZHGE and ZSP) was found to be sensitive to the discretization choice. Some of them (particularly SZSE, LGLZE and SZLGE) were also identified previously to have poor reproducibility ([23]).

In our study second-order (IDM, Inverse difference) and third-order metrics (SZSE, ZSP), previously identified as very reliable in test-retest CT ([26]) were found to be highly correlated between contrasted and non-contrasted CT scans. This result might be explained by the fact that texture analysis of both CE-CT and NCE-CT images probably reflect similar cellular distribution and these correlated features are reflecting areas of high cell density, necrosis or fibrosis, less influenced by contrast administration. Ganeshan, *et al*. found significant correlations for first order histogram features measured on CT at various scales, as well as CE-CT images, suggested that the biological correlates for heterogeneity may not be purely vascular in nature ([27]).

Radiomics' signature can be utilized as a complementary tool for the preoperative tumor staging ([28]) and has been shown to correlate with lymph nodes metastasis in colorectal cancer ([29]). In our study, Log-rank testing identified two features ($SZLGE_R$, $ZSNU_R$) to be predictive for survival on both CE and NCE- CT. Other features had prognostic power only when extracted from CE-CT ($SZLGE_{R,}$ $LGLZE_{L,}$ $LGRE_{L,}$) or only from NCE-CT ($ZSNU_R$ $GLNU_L$, $GLNU_{R,}$ $HGLZE_{E,}$ $SZHGE_L$). Amongst these features, only some derived from NCE-CT ($SZLGE_{R,}$ $SZLGE_R$,

$HGLZE_E$) were also correlated with usual clinical or pathological confounding prognostic factors. The others features may therefore provide complementary information for survival prediction.

Three categories can potentially be identified. First, highly correlated NCE-CT and CE-CT features probably reveal the same tumor heterogeneity information. Second, features found to be correlated on Spearman analysis but providing prognostic information only from either NCE-CT or CE-CT. Third, NCE-CT and CE-CT texture features that are not correlated on Spearman analysis but provide prognostic information from both modalities. Features of the two latter categories are influenced by contrast administration and should be investigated independently for the construction of predictive models as they could provide complementary prognostic information. Our results suggest that both CE-CT and NCE-CT radiomics features might be relevant for outcome prediction and tumor heterogeneity characterization when NCE-CT is available. In the era of precision medicine, these findings could be used in conjunction with biological and genomics biomarkers to help identify subgroups of patients most likely to respond to specific biologically based therapies ([30]).

Our study has several limitations. Several textural features have already shown their repeatability in other cohorts and types of cancers ([31],[32],[33]). We could not perform the reproducibility evaluation in our cohort, nor could we compare their prognostic value with that of other CT imaging modalities, since in the present cohort, only routine CT acquisitions were available. Second, the segmentation used to define tumor boundaries was realized by one expert only. This can limit the variability when considering different segmentation approaches or several observers. The segmentation tool used (3D Slicer™) has been widely used in the past to extract

robust quantitative image features, and has been employed for high throughput data mining research in clinical oncology imaging ([34]). For now, fully automated segmentation of colorectal pathologies in CT is a challenging task given the tumor complexity and low contrast with the adjacent structures. In our study, the analysis was realized on the whole tumor volume. Ng, *et al* suggested that in some tumors the largest cross-sectional area values may not be representative of the tumor as a whole and therefore the assessment of spatial heterogeneity by texture analysis on the whole tumor may best reflect the whole tumor information and overall patient survival ([7]).

Patient survival is generally related to a variety of factors, including treatment, comorbidities, diet, etc. that were not all available for analysis. These factors may potentially introduce bias into our results. Tumor markers such as CEA, CA 19-9 are not evaluated systematically in France for pre or postoperative colorectal cancer follow-up ([35]). Features and clinical variables were only assessed for prognostic value in an univariate analysis. A multivariate analysis for prognosis was out of the scope of this work, and would require a much larger cohort split into training, validation and testing. This will be addressed more thoroughly in a future work by using a larger prospective cohort, which is currently being recruited.

Conclusions

Analysis of 1st-order and textural features derived from primary colorectal tumor volume showed that most metrics are influenced by contrast administration. Some non enhanced and contrast-enhanced CT features were found to be

associated with survival while not being highly correlated between the two modalities, thus suggesting that they may provide complementary prognostic value when extracted not only from enhanced CT scans but also from non-enhanced CT scan when available. These results will be further explored in a larger prospective study.

References

1. Favoriti P, Carbone G, Greco M, Pirozzi F, Pirozzi REM, Corcione F. Worldwide burden of colorectal cancer: a review. *Updates Surg*. 2016;68(1):7-11. doi:10.1007/s13304-016-0359-y.
2. Losi L. Evolution of intratumoral genetic heterogeneity during colorectal cancer progression. 2005;26(5). doi:10.1093/carcin/bgi044.
3. Lambin P, Rios-velazquez E, Leijenaar R, et al. HHS Public Access. 2015;48(4):441-446. doi:10.1016/j.ejca.2011.11.036.Radiomics.
4. E, Segal, Sirlin CB, Ooi C, Adler AS, Gollub J, Chen X, Chan BK, Matcuk GR, Barry CT, Chang HY KM. Decoding global gene expression programs in liver cancer by noninvasive imaging. *Nat Biotechnol*. 2007;25(6):675-680. doi:10.1038/nbt1306.
5. Aerts HJ, Velazquez ER, Leijenaar RT, et al. Decoding tumour phenotype by noninvasive imaging using a quantitative radiomics approach. *Nat Commun*. 2014;5:4006. doi:10.1038/ncomms5006.
6. Tixier F, Le Rest CC, Hatt M, et al. Intratumor heterogeneity characterized by textural features on baseline 18F-FDG PET images predicts response to concomitant radiochemotherapy in esophageal cancer. *J Nucl Med*. 2011;52(3):369-378. doi:10.2967/jnumed.110.082404.
7. Ng F, Kozarski R, Ganeshan B, Goh V. Assessment of tumor heterogeneity by CT texture analysis: Can the largest cross-sectional area be used as an alternative to whole tumor analysis? *Eur J Radiol*. 2013;82(2):342-348. doi:10.1016/j.ejrad.2012.10.023.
8. Win T, Miles KA, Janes SM, et al. Tumor heterogeneity and permeability as measured on the CT component of PET/CT predict survival in patients with non-small cell lung cancer. *Clin Cancer Res*. 2013;19(13):3591-3599. doi:10.1158/1078-0432.CCR-12-1307.
9. Balaji Ganeshan, Kenneth A. Miles, Rupert C.D. Young CRC. Hepatic Enhancement in Colorectal Cancer : Texture Analysis Correlates with Hepatic Hemodynamics. 2007;(5):1520-1530. doi:10.1016/j.acra.2007.06.028.
10. Miles KA, Ganeshan B, Griffiths MR, Young RCD, Chatwin CR. Colorectal Cancer: Texture Analysis of Portal Phase Hepatic CT Images as a Potential Marker of Survival. *Radiology*. 2009;250(2):444-452. doi:10.1148/radiol.2502071879.
11. Lubner MG, Stabo N, Lubner SJ, et al. CT textural analysis of hepatic metastatic colorectal cancer: pre-treatment tumor heterogeneity correlates with pathology and clinical outcomes. *Abdom Imaging*. 2015;40(7):2331-2337. doi:10.1007/s00261-015-0438-4.

12. Cui C, Cai H, Liu L, Li L, Tian H, Li L. Quantitative analysis and prediction of regional lymph node status in rectal cancer based on computed tomography imaging. *Eur Radiol*. 2011;21(11):2318-2325. doi:10.1007/s00330-011-2182-7.
13. Liang C, Huang Y, He L, et al. The development and validation of a CT-based radiomics signature for the preoperative discrimination of stage I-II and stage III-IV colorectal cancer. *Oncotarget*. 2016;7(21):31401-31412. doi:10.18632/oncotarget.8919.
14. Edge SB, Byrd DR, Compton CC, Fritz AG, Greene FL TA. *AJCC Cancer Staging Manual (7th Ed). New York, NY:* Springer. New York, NY; 2010.
15. Parmar C, Velazquez ER, Leijenaar R, et al. Robust radiomics feature quantification using semiautomatic volumetric segmentation. *PLoS One*. 2014;9(7):1-8. doi:10.1371/journal.pone.0102107.
16. Zwanenburg, Alex; Leger, Stefan; Vallières, Martin; Löck, Steffen; Image Biomarker Standardisation Initiative for the. Image biomarker standardisation initiative. *eprint arXiv:161207003*. 2016arXiv161207003Z.
17. Sollini M, Cozzi L, Antunovic L, Chiti A, Kirienko M. PET Radiomics in NSCLC: State of the art and a proposal for harmonization of methodology. *Sci Rep*. 2017;7(1):1-15. doi:10.1038/s41598-017-00426-y.
18. Ganeshan B, Skogen K, Pressney I, Coutroubis D, Miles K. Tumour heterogeneity in oesophageal cancer assessed by CT texture analysis: Preliminary evidence of an association with tumour metabolism, stage, and survival. *Clin Radiol*. 2012;67(2):157-164. doi:10.1016/j.crad.2011.08.012.
19. Hatt M, Tixier F, Pierce L, Kinahan PE, Le Rest CC, Visvikis D. Characterization of PET/CT images using texture analysis: the past, the present… any future? *Eur J Nucl Med Mol Imaging*. 2017;44(1):151-165. doi:10.1007/s00259-016-3427-0.
20. Youden WJ. Index for rating diagnostic tests. *Cancer*. 1950;3(1):32-35. doi:10.1002/1097-0142(1950)3:1<32::AID-CNCR2820030106>3.0.CO;2-3.
21. Hatt M, Visvikis D, Albarghach NM, Tixier F, Pradier O, Cheze-le Rest C. Prognostic value of 18F-FDG PET image-based parameters in oesophageal cancer and impact of tumour delineation methodology. *Eur J Nucl Med Mol Imaging*. 2011;38(7):1191-1202. doi:10.1007/s00259-011-1755-7.
22. Miles KA, Ganeshan B, Griffiths MR, Young RCD, Chatwin CR. Colorectal cancer: texture analysis of portal phase hepatic CT images as a potential marker of survival. *Radiology*. 2009;250(2):444-452. doi:10.1148/radiol.2502071879.
23. Tixier F, Hatt M, Le Rest CC, Le Pogam A, Corcos L, Visvikis D. Reproducibility of Tumor Uptake Heterogeneity Characterization Through Textural Feature Analysis in 18F-FDG PET. *J Nucl Med*. 2012;53(5):693-700. doi:10.2967/jnumed.111.099127.
24. Leijenaar RTH, Nalbantov G, Carvalho S, et al. The effect of SUV discretization in quantitative FDG-PET Radiomics: the need for standardized methodology in tumor texture analysis. *Sci Rep*. 2015;5(August):11075. doi:10.1038/srep11075.
25. van Velden FHP, Kramer GM, Frings V, et al. Repeatability of Radiomic Features in Non-Small-Cell Lung Cancer [18F]FDG-PET/CT Studies: Impact of Reconstruction and Delineation. *Mol Imaging Biol*. 2016;18(5):788-795. doi:10.1007/s11307-016-0940-2.
26. Desseroit M-C, Tixier F, Weber WA, et al. Reliability of PET/CT Shape and Heterogeneity Features in Functional and Morphologic Components of Non–Small Cell Lung Cancer Tumors: A Repeatability Analysis in a Prospective Multicenter Cohort. *J Nucl Med*. 2017;58(3):406-411. doi:10.2967/jnumed.116.180919.
27. Ganeshan B, Goh V, Mandeville HC, Hoskin PJ, Miles K a. Non – Small Cell Lung

Cancer : Histopathologic Correlates for Texture. *Radiology*. 2013;266(1):326-336. doi:10.1148/radiol.12112428/-/DC1.
28. Liang C1, 2, Huang Y1, 2, He L1, 3, Chen X4, Ma Z1, 2, Dong D5, Tian J5, Liang C1 LZ. The development and validation of a CT-based radiomics signature for the preoperative discrimination of stage I-II and stage III-IV colorectal cancer. *Oncotarget*. 2016;7(21):31401-31412. doi:10.18632/oncotarget.8919.
29. Huang YQ1, Liang CH1, He L1, Tian J1, Liang CS1, Chen X1, Ma ZL1 LZ. Development and Validation of a Radiomics Nomogram for Preoperative Prediction of Lymph Node Metastasis in Colorectal Cancer. *J Clin Oncol*. 2016;34(18):2157-2164. doi:10.1200/JCO.2015.65.9128.
30. . http://www.e-cancer.fr/Patients-et-proches/Les-cancers/Cancer-du-colon/Suivi.
31. Yang J1, Zhang L2, Fave XJ2, Fried DV2, Stingo FC3, Ng CS4 CL. Uncertainty analysis of quantitative imaging features extracted from contrast-enhanced CT in lung tumors. *Comput Med Imaging Graph*. 2016;(48):1-8. doi:10.1016/j.compmedimag.2015.12.001.
32. Fried D V., Tucker SL, Zhou S, et al. Texture Features in Stage III Non-Small Cell Lung Cancer. *Int J Radiat Oncol Biol Phys*. 2014;90(4):834-842. doi:10.1016/j.ijrobp.2014.07.020.Prognostic.
33. Images CT, Hawkins S, Kim J, Goldgof DB, Gillies RJ. Tr a n s l a t i o n a l O n c o l o g y Reproducibility and Prognosis of Quantitative Features. 2014;7(1):72-87. doi:10.1593/tlo.13844.
34. Bézy-Wendling J, Kretowski M, Rolland Y, Le Bidon W. Toward a better understanding of texture in vascular CT scan simulated images. *IEEE Trans Biomed Eng*. 2001;48(1):120-124. doi:10.1109/10.900272.
35. TNCD. Cancer du côlon. 2011:1-23. http://www.lasfce.com/uploads/files/Cancer du colon 2011.pdf.
36. Haralick RM, Shanmugam K, Dinstein I. Textural Features for Image Classification. *IEEE Trans Syst Man Cybern*. 1973;SMC-3(6):610-621. doi:10.1109/TSMC.1973.4309314.
37. Desseroit M, Tixier F, Weber WA, et al. Non – Small Cell Lung Cancer Tumors : A Repeatability Analysis in a Prospective Multicenter Cohort. :1-7. doi:10.2967/jnumed.116.180919.
38. Lambin P. Radiomics Digital Phantom. *CancerData*. 2016. doi:10.17195/candat.2016.08.1.

Figure 1 Contrast and non contrast enhanced CT images

(a-c) NCE-CT and (b-d) CE-CT images of a patient with colonic adenocarcinoma

Figure 2 Kaplan Meyer survival curves

Kaplan Meyer survival curve with Log Rank for Stage

Figure 3 $Entropy_{HIST}$ and AUC distribution

$Entropy_{HIST}$ and AUC distribution on NCE-CT and CE-CT features

Figure 4 IDM and ID distribution

IDM (inverse difference moment) and ID (inverse difference) distribution using different quantization approaches (L-linear, E-equalization and R-fixed-width bins)

Figure 5 **SZSE and ZSP relationships**

Illustrations of correlative relationships of textural feature SZSE (small-zone-size emphasis) and ZSP (zone-size percentage) on different quantization approaches (L-linear, E-equalization, R-fixed-width bins)

Figure 6 $SZLGE_R$ and $ZSNU_R$ survival curves

Kaplan Meyer survival curves with Log Rank for CE and NCE-CT features $SZLGE_R$ (small-zone/low-gray emphasis) and $ZSNU_R$ (zone-size nonuniformity)

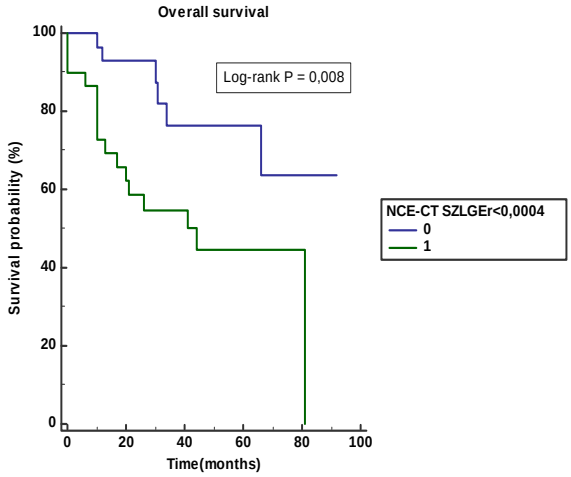
Overall survival
Log-rank P = 0,008
NCE-CT SZLGEr<0,0004
0
1
Survival probability (%)
Time(months)

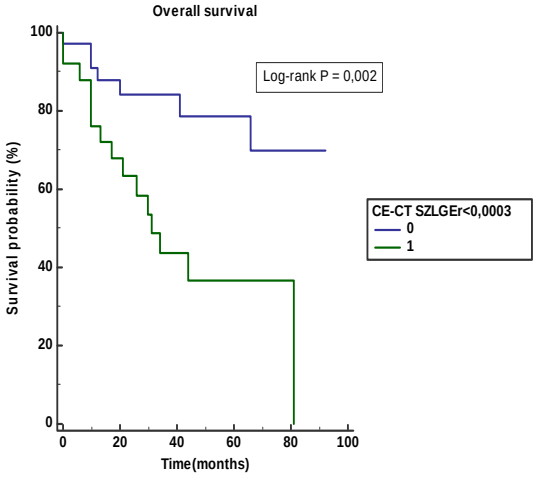
Overall survival
Log-rank P = 0,002
CE-CT SZLGEr<0,0003
0
1
Survival probability (%)
Time(months)

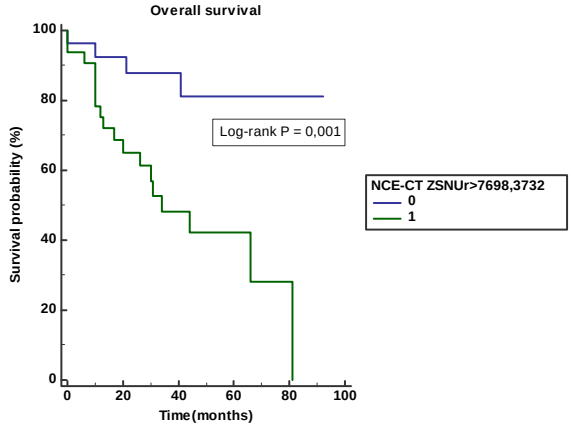
Overall survival
Log-rank P = 0,001
NCE-CT ZSNUr>7698,3732
0
1
Survival probability (%)
Time(months)

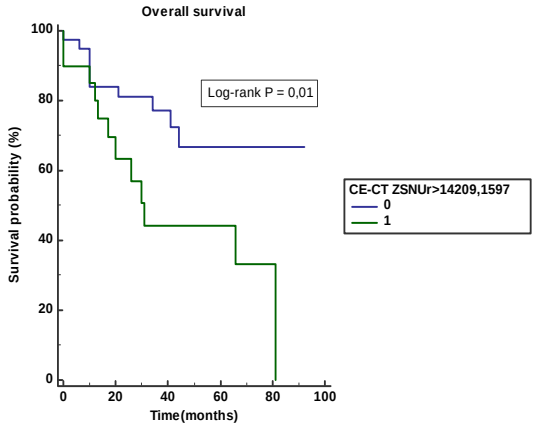
Overall survival
Log-rank P = 0,01
CE-CT ZSNUr>14209,1597
0
1
Survival probability (%)
Time(months)

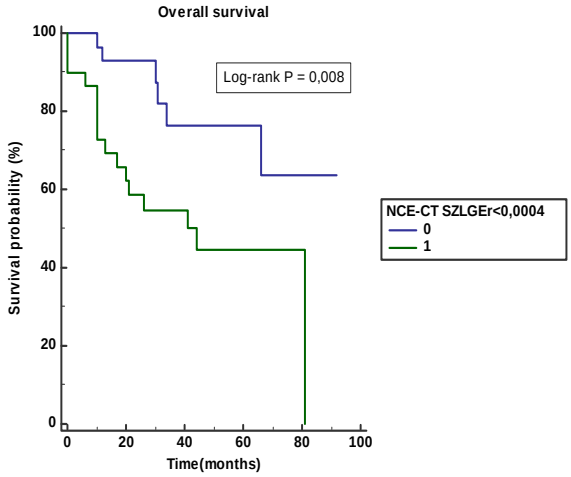
Overall survival
Log-rank P = 0,008
NCE-CT SZLGEr<0,0004
0
1
Survival probability (%)
Time(months)

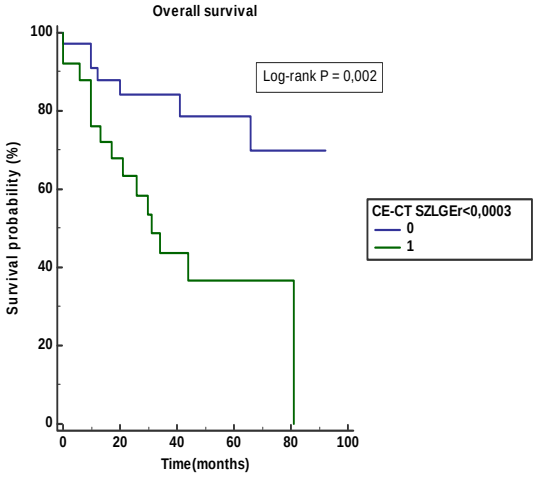
Overall survival
Log-rank P = 0,002
CE-CT SZLGEr<0,0003
0
1
Survival probability (%)
Time(months)

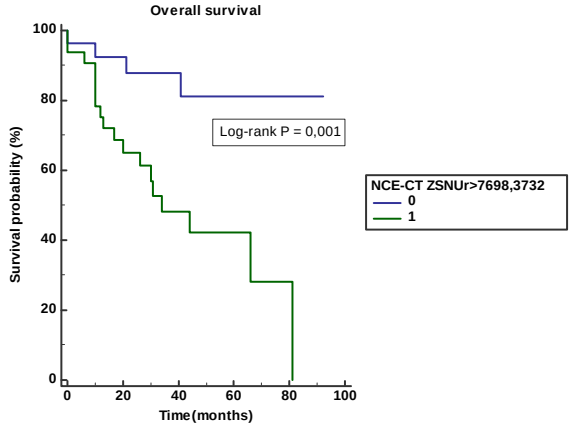
Overall survival
Log-rank P = 0,001
NCE-CT ZSNUr>7698,3732
0
1
Survival probability (%)
Time(months)

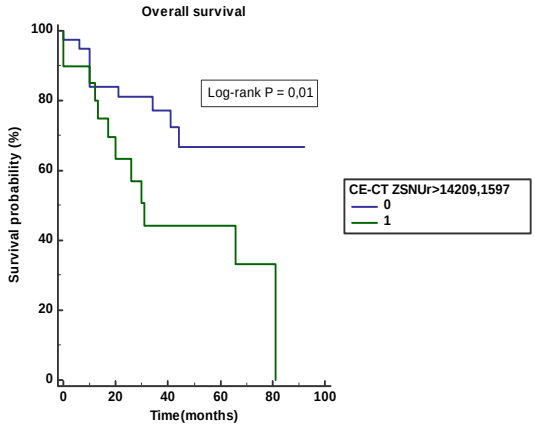
Overall survival
Log-rank P = 0,01
CE-CT ZSNUr>14209,1597
0
1
Survival probability (%)
Time(months)

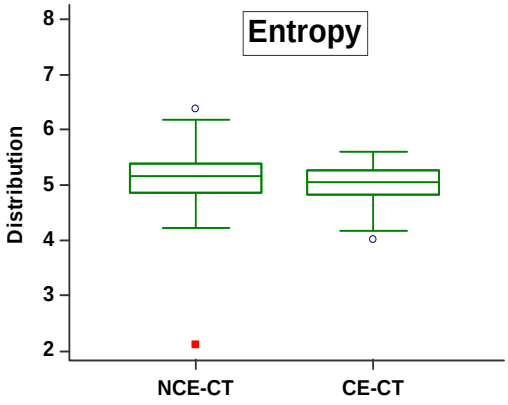
Entropy
Distribution
8
7
6
5
4
3
2
NCE-CT
CE-CT

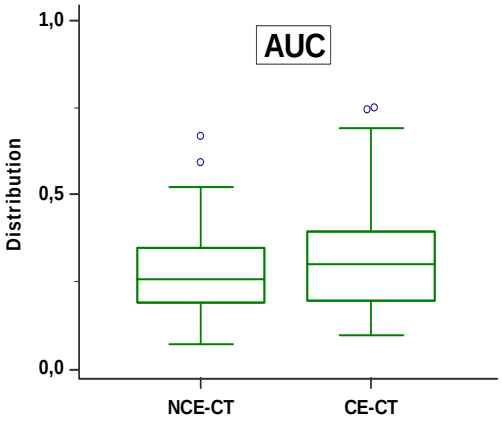
AUC
Distribution
1,0
0,5
0,0
NCE-CT
CE-CT

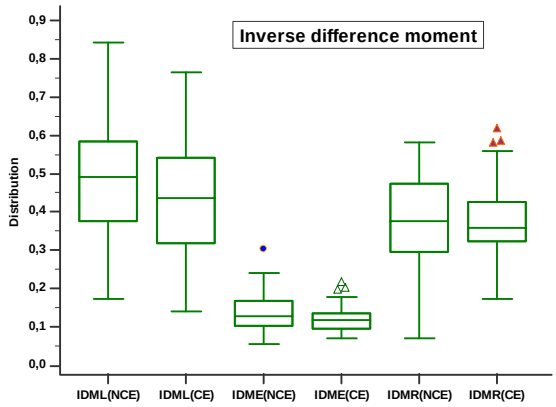
Inverse difference moment
Distribution
0,9
0,8
0,7
0,6
0,5
0,4
0,3
0,2
0,1
0,0
IDML(NCE)
IDML(CE)
IDME(NCE)
IDME(CE)
IDMR(NCE)
IDMR(CE)

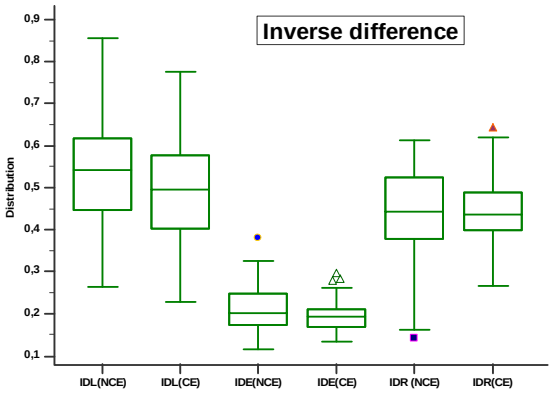
Inverse difference
Distribution
0,9
0,8
0,7
0,6
0,5
0,4
0,3
0,2
0,1
IDL(NCE)
IDL(CE)
IDE(NCE)
IDE(CE)
IDR (NCE)
IDR(CE)

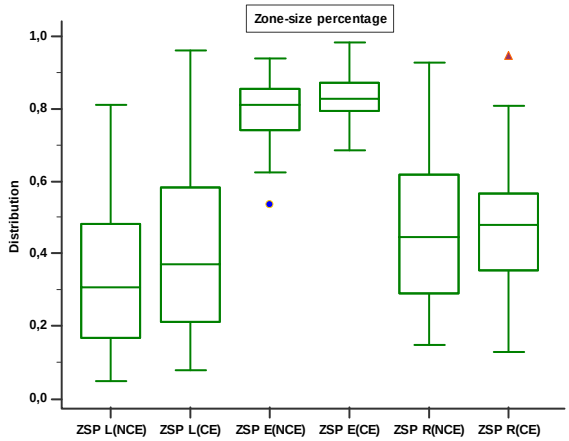
Zone-size percentage
Distribution
1,0
0,8
0,6
0,4
0,2
0,0
ZSP L(NCE)
ZSP L(CE)
ZSP E(NCE)
ZSP E(CE)
ZSP R(NCE)
ZSP R(CE)

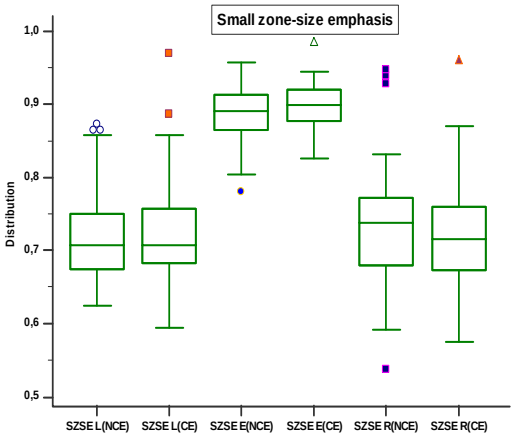
Small zone-size emphasis
Distribution
1,0
0,9
0,8
0,7
0,6
0,5
SZSE L(NCE)
SZSE L(CE)
SZSE E(NCE)
SZSE E(CE)
SZSE R(NCE)
SZSE R(CE)

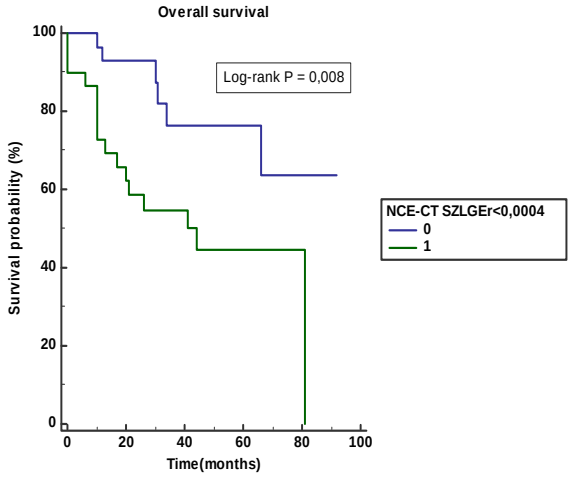
Overall survival
Log-rank P = 0,008
NCE-CT SZLGEr<0,0004
0
1
Survival probability (%)
Time(months)

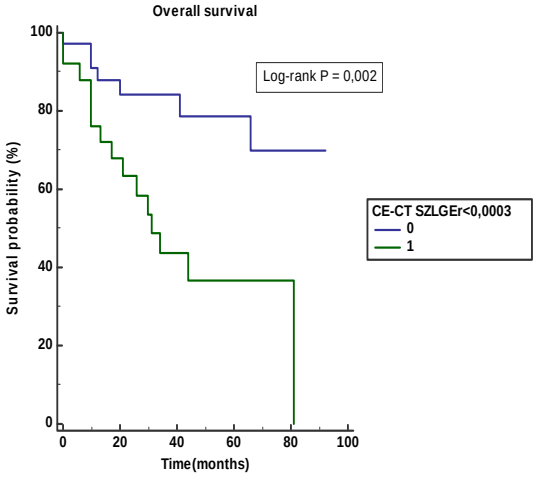
Overall survival
Log-rank P = 0,002
CE-CT SZLGEr<0,0003
0
1
Survival probability (%)
Time(months)

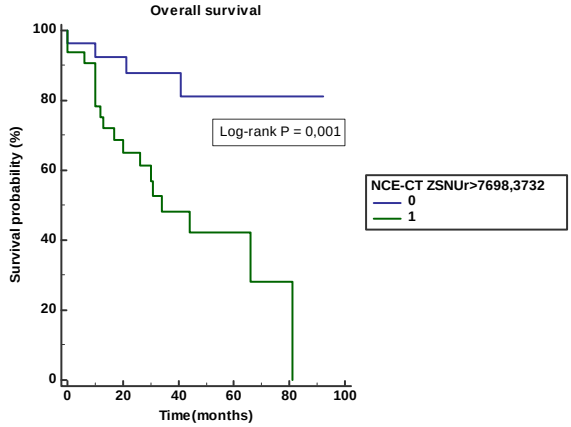
Overall survival
Log-rank P = 0,001
NCE-CT ZSNUr>7698,3732
0
1
Survival probability (%)
Time(months)

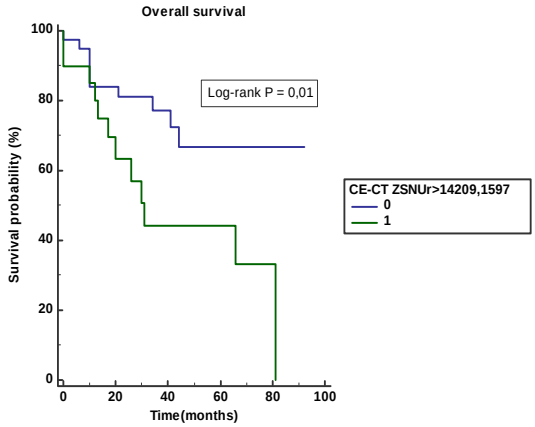
Overall survival
Log-rank P = 0,01
CE-CT ZSNUr>14209,1597
0
1
Survival probability (%)
Time(months)

Table 1. ROC analysis and Log-rank test p-values for clinical parameters

	Area under the ROC curve (AUC)	AUC P value	Log-rank test p-values
Age	0,665	0,0337	0,0016
T	0,724	0,0001	< 0,0001
N	0,576	0,2912	0,3464
M	0,663	0,0072	0,0002
R	0,626	0,0125	< 0,0001
Stage	0,721	0,0006	0,0013
Lymphovascular Invasion	0,67	0,0073	0,0004
Histologic Grade	0,548	0,5006	0,3167

T-tumor,M-metastasis,N-node,R-resection(R0 corresponds to resection for cure or complete remission. R1 to microscopic residual tumor, R2 to macroscopic residual tumor)

Table 2. Spearman rank correlation between CE and NCE CT first order features [after Holm-Bonferonni correction (*p-value* <0.000641 (=0.05/78)]

Features	Discretization	Spearman rank correlation	Spearman p-value	Log-rank	
				NCE-CT p-value	CE-CT p-value
1st order metrics					
Maximum	**N/A**	**0,434**	**0,00048**	ns	ns
Median	N/A	0,264	0,04005*	ns	ns
Standard Deviation	N/A	0.367	0.003653*	ns	ns
Skewness	**N/A**	**0,511**	**0,00003**	ns	ns
Kurtosis	N/A	0,318	0,01250*	ns	ns
Entropy$_{HIST}$	**N/A**	**0.491**	**0.0000580**	ns	ns
AUC	**N/A**	**0.413**	**0.0000580**	ns	ns

AUC- area under curve; E- equalization ID - inverse difference; L-linear discretization;; R-resampling; ns- not significant;*-not significant after Bonferroni p-value correction

Table 3. Spearman rank correlation between CE and NCE CT second order features [after Holm-Bonferonni correction (*p-value* <0.000641 (=0.05/78)]

Features	Discretization	Spearman rank correlation	Spearman p-value	Log-rank	
				NCE-CT	CE-CT
				p-value	p-value
2nd order metrics					
ASM	L	0,399	0,00145*	ns	ns
	E	**0.595**	**0.0000004**	ns	ns
	R	**0,626**	**0,00000**	ns	ns
Contrast$_{GLCM}$	L	0,312	0,01435*	ns	ns
	E	**0.555**	**0.0000035**	ns	ns
	R	**0,463**	**0,00017**	ns	ns
SOSV	**L**	**0,477**	**0,00010**	ns	ns
	E	0.100	ns	ns	ns
	R	**0.535**	**0.0000089**	ns	ns
IDM	L	0,377	0,00277*	ns	ns
	E	**0.610**	**0.0000002**	ns	ns
	R	**0.742**	**0.0000000**	0,093	ns
SAVE	**L**	**0,444**	**0,00034**	ns	ns
	E	0.187	ns	ns	ns
	R	**0.543**	**0.0000062**	ns	ns
SVAR	L	0,244	ns	ns	ns
	E	**0.528**	**0.0000120**	ns	ns
	R	0.285	0.0260644*	ns	ns
SENT	**L**	**0.434**	**0.0004700**	0,0067	ns
	E	**0.551**	**0.0000042**	ns	ns
	R	0.411	0.0009893*	ns	ns
Entropy$_{GLCM}$	L	0.426	0.0006126*	ns	ns
	E	**0.550**	**0.0000045**	ns	ns
	R	**0.600**	**0.0000003**	ns	ns
DVAR	L	0,343	0,00680*	ns	ns
	E	**0.503**	**0.0000366**	ns	ns
	R	0.423	0.0006794*	ns	ns
DENT	L	0.393	0.0017372*	ns	ns
	E	**0.580**	**0.0000009**	ns	ns
	R	**0.624**	**0.0000001**	ns	ns
Autocorrelation	**L**	**0,471**	**0,00013**	ns	ns
	E	**0.462**	**0.0001797**	ns	ns
	R	**0.536**	**0.0000085**	ns	ns
Dissimilarity	L	0,333	0,00879*	ns	ns
	E	**0.590**	**0.0000006**	ns	ns

	R	**0.600**	**0.0000003**	ns	ns
Prominence	L	0,271	0,03485*	ns	ns
	E	**0.502**	**0.0000371**	ns	ns
	R	0.362	0.0041615*	ns	ns
ID	L	0,374	0,00296*	ns	ns
	E	0.214	ns	ns	ns
	R	**0.724**	**0.0000000**	0,0532	ns

E- equalization; ID - inverse difference; L-linear discretization; R-resampling; SAVE - sum average; SENT - sum entropy; SOSV - sum of square variance; SZSE- Small Zone Size Emphasis, LZSE- Large Zone Size Emphasis, HGLZE-High Grey Level Zone Emphasis, SZLGE- Small Zone / Low Grey Emphasis, SZHGE- Small Zone / High Grey Emphasis, LZLGE- Large Zone / Low Grey Emphasis, SZP- Zone Size Percentage;

ns- not significant;*-not significant after Bonferroni p-value correction; Bold values-significant correlations rs>0.7